

Behaviour of Natural and Implanted Iron during Annealing of Multicrystalline Silicon Wafers

Daniel Macdonald^{1,a}, Thomas Roth^{1,b}, L. J. Geerligs^{2,c} and Andres Cuevas^{1,d}

¹ Department of Engineering, The Australian National University, Canberra 0200 ACT, Australia

² Energy Research Centre of the Netherlands (ECN), PO Box 1, NL-1755 ZG Petten, The Netherlands

^aDaniel.Macdonald@anu.edu.au, ^bthomas.roth@ise.fraunhofer.de, ^cgeerligs@ecn.nl, ^dAndres.Cuevas@anu.edu.au

Keywords: crystalline silicon, iron, precipitates, recombination

Abstract. Changes in the concentration of interstitial iron in multicrystalline silicon wafers after high temperature annealing (900°C) have been monitored by carrier lifetime measurements. Two cooling rates were investigated. The first was considered ‘fast’, meaning the interstitial Fe had no time to diffuse to precipitation sites, and should therefore be frozen-in, despite being far above the solubility limit at lower temperatures. A second ‘slow’ cool down to 650°C allowed ample time for the Fe to reach the surfaces or other internal precipitation sites. Surprisingly, in both cases the Fe remained in a supersaturated state. This indicates the precipitation process is not diffusion-limited, and that another energetic barrier to precipitate formation must be present. Since the slow cooling used here is similar to the cooling rate experienced by multicrystalline ingots after crystallisation, this precipitate-impeding mechanism is probably responsible for the surprisingly high interstitial Fe concentrations often found in as-grown multicrystalline silicon wafers.

Introduction

Iron is a common impurity in multicrystalline silicon (mc-Si) for solar cells, and can occur as interstitial iron (Fe_i) or as precipitates [1-4]. Both forms can impact on cell performance, although to differing degrees, and may transform from one to the other during high temperature steps. Hence the behaviour of Fe during ingot growth and subsequent cell processing is an important issue in photovoltaics.

The very slow cooling of mc-Si ingots after crystallisation provides an ideal climate for Fe precipitation, while the relatively rapid cooling typical after cell process steps is more likely to ‘freeze-in’ any Fe present in interstitial form at high temperatures. In this work we have attempted to mimic these two cooling regimes in a quartz furnace, using mc-Si wafers with a large range of starting Fe concentrations. Monitoring how the interstitial Fe concentration changes, while also considering changes in the solubility limit and Fe diffusivity during the process steps, allows some insight into the mechanisms which control the formation and dissolution of Fe precipitates.

Experimental Details

In this work we have studied iron, both naturally occurring and deliberately introduced, in multicrystalline silicon (mc-Si) wafers from the central part of two directionally-solidified ingots from different manufacturers, labelled S and P. Two sets of wafers from each ingot were chosen, with one set subjected to phosphorus gettering prior to further processing and analysis. This results in a dramatic drop in the naturally occurring interstitial Fe (Fe_i) concentration in these wafers, providing samples with significantly different Fe_i concentrations. Phosphorus gettering was performed in a quartz furnace containing POCl₃ vapour at a temperature of 880°C for 1 hour. After gettering, the heavily diffused region was etched off prior to further processing.

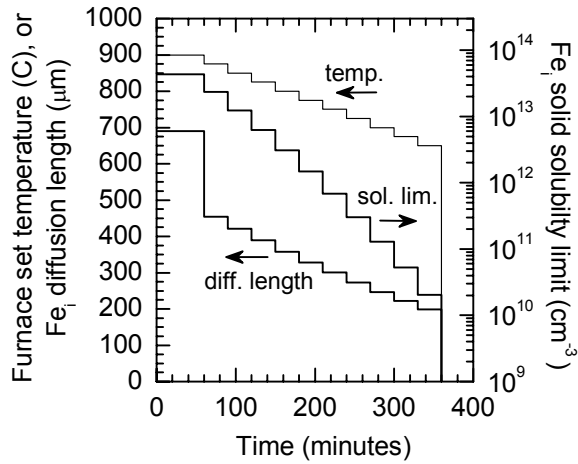


Figure 1. Temperature profile for the slow-cooled samples. Also shown are the solid solubility limits and the diffusion lengths for Fe_i at each temperature step.

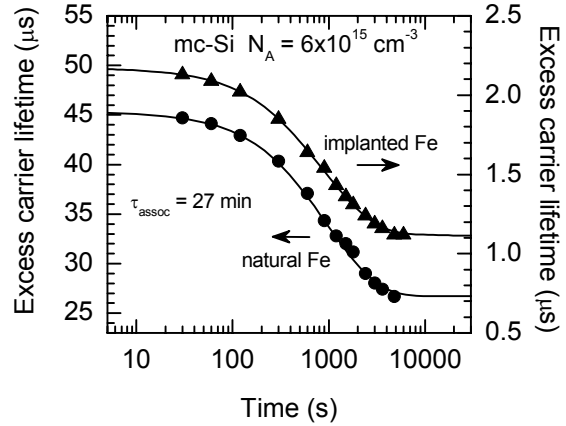


Figure 2. Decrease in carrier lifetime (at $\Delta n = 5 \times 10^{15} \text{ cm}^{-3}$) as the FeB pairs re-form after illumination ($T = 31^\circ\text{C}$). An exponential fit (solid line) gave an identical re-pairing time τ_{assoc} of 27 minutes for mc-Si samples containing implanted or 'natural' Fe_i .

Some wafers from both ingots, including gettered and non-gettered samples, plus some float-zone single-crystal controls, were then implanted with Fe. This allows a third, considerably higher Fe_i concentration to be achieved. Implants were performed at a relatively low energy of 70 keV and a dose of $5 \times 10^{11} \text{ cm}^{-2}$. All of the implanted samples, along with a selection of the non-implanted samples, were then annealed at 900°C for 1 hour in a nitrogen atmosphere. This allows the implanted Fe to distribute itself quite uniformly throughout the wafer thickness, as the diffusion length of Fe is approximately 700 microns [5] during this anneal step, in comparison to the sample thicknesses of between 160 and 300 microns. Note also that the solubility limit of Fe at 900°C is around $4.3 \times 10^{13} \text{ cm}^{-3}$ [5], which is above the volume concentration of Fe corresponding to the implant dose used for all samples ($[Fe] = \text{dose}/\text{thickness} = 3.1 \times 10^{13} \text{ cm}^{-3}$ for the thinnest implanted wafer). Hence there should be no significant precipitation of Fe while the samples are held at 900°C . Another important point to note is that the crystal damage associated with this low energy and dose is known to be very effectively healed after such an annealing step, leaving no detectable recombination centres [6]. If such defects were present, they could mask the effect of the Fe atoms through their recombination activity, or act as precipitation sites through relaxation-gettering [7].

The principal aim of this experiment was to observe the behaviour of Fe during fast or slow cooling from high temperature, during which time the solubility limit is exceeded. Hence, one set of samples annealed as above were 'fast-cooled', meaning that they were extracted from the quartz furnace directly into air, as might occur during typical device processing. A second set were 'slow-cooled' by ramping the furnace down in steps of 25°C every 30 minutes until 650°C was reached, a total cooling time of 5 hours. This is more representative of the cooling rate experienced during cooling after ingot growth. Figure 1 shows the target temperature during the slow-cool ramp down (the real temperature profile would have been smoother), as well as Fe_i solid solubility limit in intrinsic silicon [5] at each temperature and the Fe_i diffusion length L ($L = (D_{Fe} \times t)^{0.5}$) [5] of Fe_i for each 30 minute step. The figure shows that the solubility limit is massively exceeded at the lower temperatures for the implanted samples, while the diffusion length is still sufficiently long for the Fe_i to reach the surfaces and other precipitation sites. This is important, since iron is known to precipitate heterogeneously [8], in other words, it requires such extrinsic defects to trigger precipitate formation. Consequently, extensive precipitation might be expected in such slow-cooled samples.

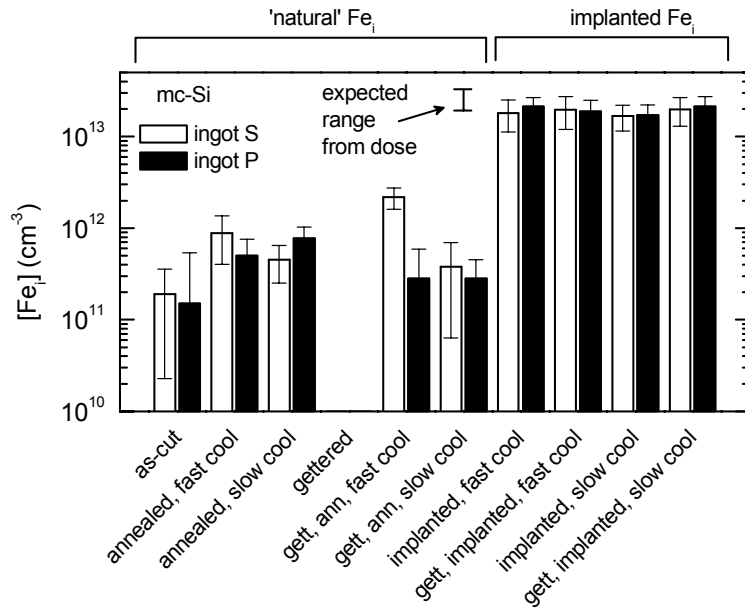


Figure 3. Fe_i concentrations in the multicrystalline samples for the 2 ingots. For the implanted samples (at right) the expected Fe_i concentration is the dose divided by the wafer thickness.

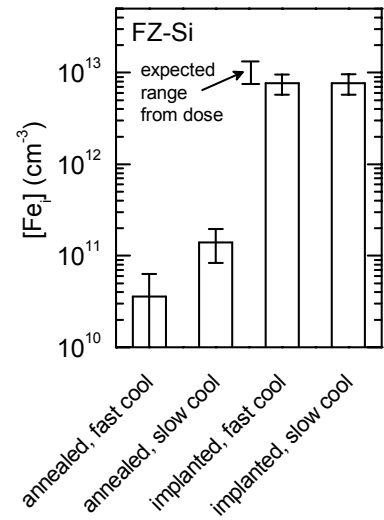


Figure 4. Fe_i concentrations in the FZ samples.

After annealing and cooling, the surfaces of the samples were passivated with plasma-enhanced chemical-vapour-deposited SiN layers at 400°C [9]. The excess carrier lifetimes were then measured with the quasi-steady-state photoconductance (QSSPC) technique [10], before and after illumination with strong white light (approximately 100 mW/cm²) for 2 minutes. The illumination causes FeB pairs to break, resulting in a change in the carrier lifetime [11]. For a given base doping level and excess carrier concentration Δn (in this case we used $\Delta n = 1 \times 10^{15}$ cm⁻³), the interstitial Fe concentration $[Fe_i]$ can be calculated from the change in lifetime, down to values as low as 10¹⁰ cm⁻³ [12].

There are two independent ways of confirming that the lifetime changes are indeed due to Fe contamination. Firstly, the rate at which the lifetime recovers after illumination back to the initial value depends on the doping concentration and the diffusivity of Fe_i at room temperature. This characteristic association time of the FeB pairs τ_{assoc} is reasonably well known [11]. The values we measured for both the implanted and non-implanted mc-Si samples, as shown in Figure 2, were identical to one another ($\tau_{assoc} = 27$ min), confirming that the non-implanted sample does indeed contain Fe. They are also comparable in magnitude to the expression in Ref. [11] ($\tau_{assoc} = 65$ min), the factor of two difference being consistently observed in Fe-doped samples in our laboratories, and which will be the subject of a forthcoming publication. Secondly, in all cases we observed the characteristic ‘crossover’ point at an excess carrier density near 1 × 10¹⁴ cm⁻³ that has recently been shown to be characteristic of Fe_i in crystalline silicon of similar base doping concentration [12].

Results and Discussion

The measured values of $[Fe_i]$ are shown in Figures 3 and 4 for the mc-Si and FZ samples respectively. On the left-hand side of Figure 3, the mc-Si samples containing only ‘natural’ Fe are shown. The error bars are calculated assuming an uncertainty of 10% in the lifetime measurements. The first observation is that even in the ‘as-cut’ state, meaning no gettering or annealing, there is approximately 1–2 × 10¹¹ cm⁻³ of Fe_i for both the mc-Si ingots. These values are similar to previous observations for wafers from the centre of mc-Si ingots [2–4]. However, after phosphorus gettering, this has been reduced to below the detection limit (about 5 × 10¹⁰ cm⁻³), indicating effective and deep

gettering. This is to be expected considering the long gettering time (60 minutes), during which the diffusion length of Fe is around 700 microns. The effective lifetimes measured before and after gettering, with any interstitial Fe in the paired state, increased from 38 to 55 μs for ingot S, and from 22 to 130 μs for ingot P.

However, upon annealing at 900°C for 1 hour, the Fe_i concentration increases again. Note that this increase is quite clearly not due to processing contamination, since the co-processed FZ controls contained significantly less Fe_i , as shown in Figure 3 (the slow cooled FZ had a little more Fe present, probably because the longer time in the furnace allowed more contamination). Therefore the increased Fe_i concentration in the mc-Si wafers must come from within the wafers themselves, with the most likely source being the slow dissolution of Fe precipitates. These are known to exist in mc-Si [13], and account for the vast majority of the total Fe content in the material, which is typically in the 10^{13} - 10^{14} cm^{-3} range [1,4]. Note however that the small fraction of Fe in interstitial form, approximately 10^{11} - 10^{12} cm^{-3} in these wafers, is more active in terms of recombination. The fact that the Fe_i concentrations after annealing are similar in both the gettered and non-gettered samples suggests that the previous gettering step had not depleted these precipitates to a significant extent. This is consistent with the fact that the amount of Fe_i removed by the gettering is apparently very small compared to the total concentration of Fe stored in precipitates.

Interestingly, the results for the non-implanted mc-Si wafers after annealing are the same for either the fast or slow cooling. This is somewhat unexpected, since during the latter stages of the slow cool, the solubility limit of Fe_i is well below the concentrations measured (see Figure 1). The lack of precipitation is even more obvious in the implanted samples, shown on the right of Figure 3 for the mc-Si wafers, and in Figure 4 for the FZ samples. Note that the implanted mc-Si samples all have the same values of $[\text{Fe}_i]$, since the implanted concentration far exceeds the ‘natural’ concentrations. Despite the Fe_i concentration in the implanted samples being almost 3 orders of magnitude higher than the solubility limit at 650°C, all of the Fe apparently remains interstitial! This is true for both the FZ and mc-Si samples, despite the presence of the surfaces as precipitation sites in the FZ, as well as many internal extrinsic defects in the mc-Si. These results imply that there may exist an energetic barrier to precipitate formation, resulting in a supersaturated state. Alternatively, the solubility limit in these moderately boron-doped wafers (around 1 Ωcm) may be much greater than in intrinsic material, which was used to determine the solubilities [5]. This latter explanation seems unlikely however, since the solubility of metals is usually only significantly affected by the doping concentration in p-type silicon if the latter is in the 10^{19} - 10^{20} cm^{-3} range [14]. The supersaturation of Fe observed in these samples is reminiscent of, and corroborated by, the mysterious fact that measurable quantities of Fe_i almost always exist in as-grown mc-Si material, despite the extremely slow ingot cooling that should result in almost complete precipitation.

Comparable studies of Fe precipitate formation in FZ silicon in the temperature range from 300 to 800°C were performed by Henley and Ramappa [15]. At 700°C, after 30 minutes annealing, they observed a slight reduction in $[\text{Fe}_i]$ from an initial value of around 3×10^{13} down to $1\text{-}2 \times 10^{13}$ cm^{-3} . The latter value is similar to those observed here after annealing at 650°C. Hence their results also indicated a supersaturated state that persisted longer than expected on the basis of the diffusivity of Fe. Interestingly, Henley and Ramappa found that precipitate formation was most pronounced for anneals around 500°C, when $[\text{Fe}_i]$ dropped by more than 2 orders of magnitude to around 1×10^{11} cm^{-3} after 90 minutes. This is somewhat surprising, since the solubility is already extremely low at considerably higher temperatures, where the barrier to precipitation is presumably more easily overcome. It may be that the competing mechanism of precipitate dissolution plays a role at temperatures above 600°C. Future work will examine the rate of precipitation in mc-Si wafers at these lower temperatures around 500°C, and attempt to determine activation energies of precipitate formation and dissolution in this material.

It seems that during the slow cooling after growth of multicrystalline silicon ingots, the majority of the Fe precipitation occurs at relatively low temperatures below 650°C. In principle it

could be possible to make use of this precipitation by holding ingots at around 500°C for extended periods during ingot cooling. This should result in more complete Fe precipitation. However, this may be of limited value, since these precipitates are likely to be partially dissolved at higher temperatures during cell processing, in analogy to the pre-gettered wafers of this study.

Conclusions

There are two aspects to the results obtained in this work, one relating to the behaviour of Fe at high temperature, and the other to its precipitation, or lack thereof, during cooling.

Firstly, the interstitial Fe concentration in mc-Si, typically around 10^{11}cm^{-3} in ‘as-cut’ wafers from the centre of an ingot, can increase during annealing at high temperatures (around 900°C), due to the dissolution of precipitates. If the released Fe is not subsequently gettered by doped layers or passivated by hydrogen, it may degrade cell performance. Our pre-gettering step does not appear to be sufficient to deplete these precipitates to a large extent.

Secondly, during cooling from high temperature, the interstitial Fe remains in a highly supersaturated state down to 650°C. This occurs despite the fact that the solubility is very low and the diffusion length of Fe is more than long enough to reach the surfaces, or other precipitation sites, which must be common in the mc-Si. This latter observation suggests that the precipitation process is not diffusion-limited, but rather is impeded by some energetic barrier to precipitate formation.

Acknowledgements

This work has been supported by the Australian Research Council and The Netherlands Agency for Energy and the Environment (NOVEM). The authors are grateful to H. Tan, C. Jagadish and R. Elliman of the Dept. of Electronic Materials Engineering, Research School of Physical Sciences and Engineering, ANU, for access to the PECVD reactor and ion-implanter.

References

- [1] A.A. Istratov, *et al.*: J. Appl. Phys. Vol. 94 (2003), p. 6552.
- [2] L.J. Geerligs: Proceedings of the 3rd World Conference on Photovoltaic Solar Energy Conversion, Osaka (WCPEC-3, 2003), p. 1044.
- [3] R.A. Sinton, T. Mankad, S. Bowden and N. Enjalbert: Proceedings of the 19th European Photovoltaic Solar Energy Conversion Conference, Paris (WIP-Munich, 2004), p. 520.
- [4] D. Macdonald, A. Cuevas, A. Kinomura, Y. Nakano and L.J. Geerligs: J. Appl. Phys. Vol. 97 (2005), p. 033523.
- [5] A.A. Istratov, H. Hieslmair and E.R. Weber: Appl. Phys. A Vol. 69 (1999), p. 13.
- [6] D. Macdonald, P.N.K. Deenapanray and S. Diez: J. Appl. Phys. Vol. 96 (2004), p. 3687.
- [7] A.A. Istratov, W. Huber and E.R. Weber: Appl. Phys. Lett. Vol. 85 (2004), p. 4472.
- [8] K. Graff: *Metal Impurities in Silicon-Device Fabrication* (Springer-Verlag, Berlin 2000).
- [9] M.J. Kerr and A. Cuevas: Semicond. Sci. Technol. Vol. 17 (2002), p. 166.
- [10] R.A. Sinton and A. Cuevas: Appl. Phys. Lett. Vol. 69 (1996), p. 2510.
- [11] G. Zoth and W. Bergholz: J. Appl. Phys. Vol. 67 (1990), p. 6764.
- [12] D. Macdonald, L.J. Geerligs and A. Azzizi: J. Appl. Phys. Vol. 95 (2004), p. 1021.
- [13] T. Buonassisi, *et al.*: J. Appl. Phys. Vol. 97 (2005), p. 074901.
- [14] A.A. Istratov, *et al.*: J. Appl. Phys. Vol. 97 (2005), p. 023505.
- [15] W.B. Henley and D.A. Ramappa: J. Appl. Phys. Vol. 82 (1997), p. 589.